STM JOURNALS

Research & Reviews: Journal of Physics
ISSN: 2278-2265(online), ISSN: 2347-9973(print)
Volume 4, Issue 2
www.stmjournals.com

Kinetics of Non-isothermal Crystallization of Ge-Se-Sn Chalcogenide Glasses

Anusaiya Kaswan*, Vandana Kumari, D. Patidar, N.S. Saxena, Kananbala Sharma
Semi-conductor & Polymer Science Laboratory, Department of Physics, University of Rajasthan, Jaipur, Rajasthan, India

Abstract

The calorimetric measurements of as-prepared $Ge_{30-x}Se_{70}Sn_x$ ($8 \leq x \leq 20$) chalcogenide glasses have been performed using differential scanning calorimetery (DSC) at five different heating rates (10, 15, 20, 25 and 30 $Kmin^{-1}$) under non-isothermal conditions. These non-isothermal calorimetric measurements have been analyzed in terms of activation energy (E_c), Avrami exponent, dimensionality of growth, frequency factor, $K_o(sec^{-1})$, half time of crystallization,$t_{1/2}$(min) and crystallization rate parameter. These kinetic parameters have been evaluated using different theoretical approaches such as; Kissinger model, Ozawa model, Augis-Bennett, Matusita model, Gao-Wang model, Avrami model and Mo's approach. It has been observed that the activation energy of crystallization E_c ($KJmole^{-1}$) is composition dependent. The activation energy decreases with increasing Sn content due to the decreasing rate of crystallization. It has also been observed that the half-time of crystallization decreases with increasing heating rate because when heating rate increases crystallization rate become faster.

Keywords: *Avrami exponent, Half-time of crystallization, Frequency factor*

****Author for Correspondence*** E-mail: anu.spsl@gmail.com

INTRODUCTION

Amorphous alloys are relatively new materials offering a specific combination of technologically important properties and have thus attracted special interest of material scientists in the last few decades. Glasses also have amorphous nature. These materials are structurally and thermodynamically metastable and very susceptible to partial or complete crystallization during thermal treatment or during their applications. The glass-forming region in the ternary Ge-Se-Sn system extends to about 20 at. %Sn and about 22 at. %Ge, with the rest being Se. The freedom allowed in the preparation of glasses in varied compositions brings about changes in their short-range order and thus results in variations in their physical properties [1]. Therefore, it is possible to tailor their various properties to a desired technological application. The applications of these glassy alloys include a very wide spectrum such as computer memories, erasable high-density optical memories [2–6]. These chalcogenide glasses are being studied mostly for photoconductive applications such as; photoreceptors in copying machines and x-ray imaging plates, IR optical lenses, windows and high sensitivity ionic sensors [7–11]. The kinetics of crystallization of chalcogenide glasses plays an important role in determining the transport mechanism, thermal stability and practical applications. In this regard this paper reports the non-isothermal crystallization kinetics in terms of activation energy and thermal stability. Besides, half-time of crystallization and crystallization rate factor have also been investigated using the volume of fraction crystallized (X)-time curves for Ge-Se-Sn system with different percentage of Sn content. Both Avrami model and Mo approach (which is combined form of two isothermal approaches, Avrami model and Ozawa model) have also been applied to obtain the information about Avrami exponent and crystallization rate parameters.

EXPERIMENTAL DETAILS

The appropriate atomic weight percent proportions of the constituent elements (high purity (99.999%) germanium, selenium and tin) were weighed and the weighed materials

were then introduced into clean quartz ampoule. The contents of the ampoule (length 5 cm and internal diameter 8 mm) were sealed under a vacuum of 10^{-6} torr and then heated in furnace where temperatures were raised at a rate of 3–4 $Kmin^{-1}$ up to 925˚C. The contents were kept around that temperature for 12–14 h with continuous rotation to ensure the homogeneity of the sample. The molten sample was quickly quenched in ice- cooled water to get glassy state. The ingots of so produced glassy samples were taken out of the ampoule by breaking the ampoule and then grinded gently in mortar and pestle to obtain them in powder form.

The amorphous nature of glassy alloys was ascertained with X-ray diffraction (XRD). The XRD measurements were processed by Bragg-Brentano geometry on a Panalytical X'pert diffractometer with a Cu K_α radiation source (1.5406Å). Figure 1 shows the XRD diffractograms of the Ge_{30-x} $Se_{70}Sn_x$ ($8 \leq x \leq 20$) glassy materials. The calorimetric measurements were carried out using differential scanning calorimetery Rigaku (DSC-8230) with an accuracy of ± 0.1 K. 10 mg-powdered samples were crimped into aluminium pans and scanned at different heating rates (10, 15, 20, 25 and 30 $Kmin^{-1}$). Figure 2 shows the DSC thermograms of $Ge_{13}Se_{70}Sn_{17}$ chalcogenide glass at different heating rates (10, 15, 20, 25 and 30 $Kmin^{-1}$). To evaluate the transformed portion of the amorphous material, partial area analysis of the DSC peaks had been used.

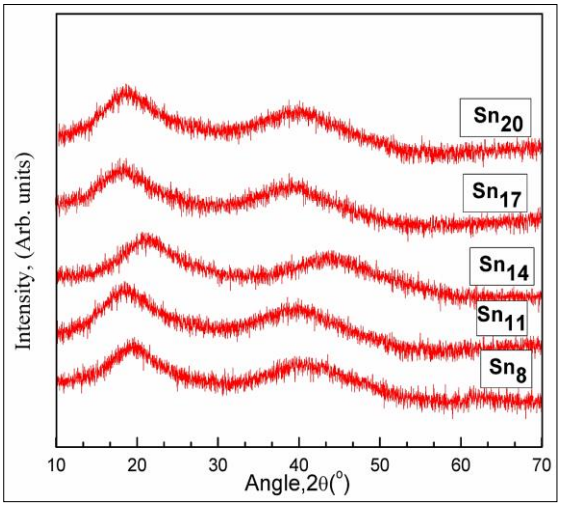

Fig. 1: *XRD Diffractograms of the $Ge_{30-x}Se_{70}Sn_x$ ($8 \leq x \leq 20$) Glassy Materials.*

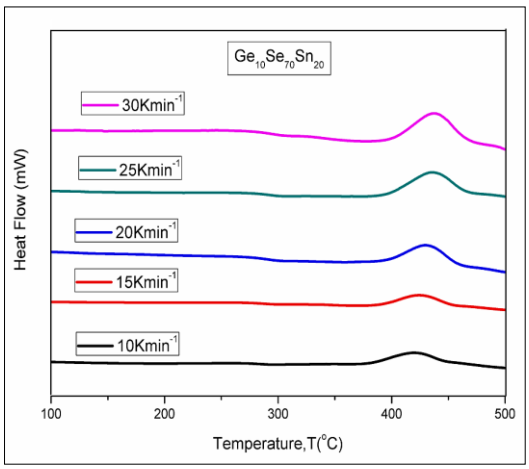

Fig. 2: *DSC Thermograms of $Ge_{13}Se_{70}Sn_{17}$ with Different Heating Rates (10, 15, 20, 25 and 30 $Kmin^{-1}$).*

RESULTS AND DISCUSSION

The non-isothermal crystallization kinetics of Ge-Se-Sn system has been studied in terms of activation energy, Avrami exponent (n_o), dimensionality of growth (m), frequency factor (K_o) and analysis of variation of volume of fraction crystallized (X) with time of crystallization.

ACTIVATION ENERGY (E_C)

The activation energy is an important parameter since it indicates the thermal stability of glasses and its magnitude reflects the nature of the transformation. The activation energy of the glass crystallization is associated with nucleation and growth processes. It is generally known that onset crystallization temperature is strongly associated with nucleation process and the peak crystallization temperature is related to the growth process. Therefore, the activation energy calculated from onset crystallization temperature represents the activation energy for nucleation E_n and other values denote the activation energy for growth E_g [12]. It has been pointed out that in non-isothermal measurements, generally due to a rapid temperature rise and the big difference in the latent heat of nucleation and growth, the crystallization exotherm characterizes the growth of the crystalline phase from the amorphous matrix; nucleation takes place very rapidly and immediately after overheating the material in the initial stages of the crystallization exotherm which results in the deformed beginning of measured exotherm.

Accordingly, the obtained value of E_c can be taken to represent the activation energy of growth [13].The investigation of activation energy of crystallization (E_c) has been done using following theoretical isokinetic approaches:

The peak shift method of **Kissinger** is most commonly used in analyzing the crystallization data in DSC experiments under the nonisothermal conditions. The activation energy of crystallization has been calculated using this method. The mathematical formulation of Kissinger model is [14, 15]:

$$Ln\left(\frac{\beta}{T_P^2}\right) = Constant - \frac{E_c}{RT_P} \quad (1)$$

where, T_p is the peak crystallization temperature. Plots of $Ln\left(\frac{\beta}{T_P^2}\right)$ versus $1000/T_p$ are shown in Figure 3 for Ge_{30-x} $Se_{70}Sn_x$ ($8 \leq x \leq 20$) glassy samples. The curves are found to be linear for different concentration of Sn content. The activation energy of crystallization E_c is obtained from the slope of these plots and the values of E_c have been listed in Table 1.

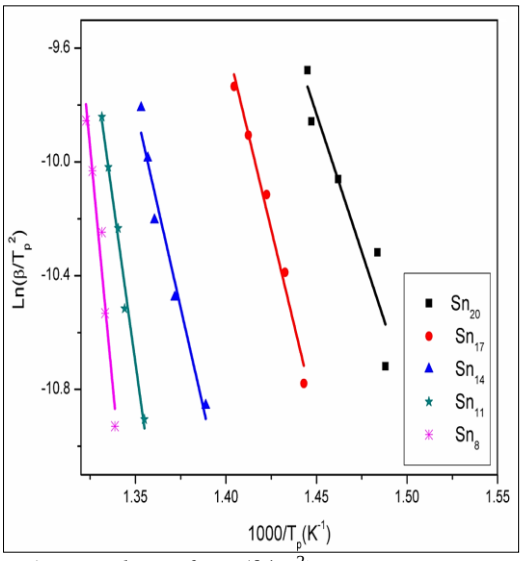

Fig. 3: *Plots of Ln (β/T_p^2) against $1000/T_p$.*

Table 1: *Values of the Activation Energy of Crystallization E_c (KJmole^{-1}) for $Ge_{30-x}Se_{70}Sn_x$ ($8 \leq x \leq 20$) Glassy Samples using Different Models.*

Sn (at%)			Ec(KJmole^{-1})		
	Kissinger	**Matusita**	**Gao-Wang**	**Ozawa**	**Anguis- Bennet**
8	242.89	243.34	263.76	233.09	259.19
11	209.78	225.09	229.13	203.43	223.79
14	200.15	221.15	212.70	195.45	207.75
17	181.73	186.08	198.91	174.01	185.65
20	161.35	149.89	179.27	121.52	160.22

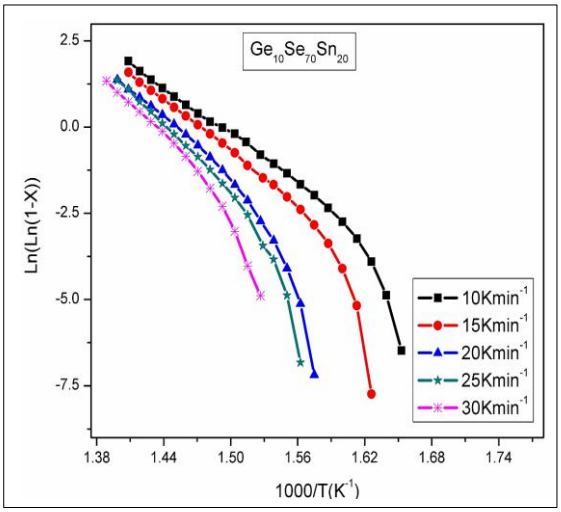

Fig. 4: *Plots of Ln (-ln(1-X)) vs. 1000/T $Ge_{10}Se_{70}Sn_{20}$ Glass.*

The activation energy of the crystallization can also be evaluated by an alternative approach given by **Matusita** model leading to the following equation [16]:

$$Ln[-Ln(1-X)] = Constant - n_o Ln\beta - 1.052\left(\frac{mE_c}{RT}\right) \quad (2)$$

where, quantity X represents the volume of fraction crystallized of the amorphous matrix at a constant heating rate at a particular temperature; m and n_o are numerical factors which reflect the nucleation process and growth morphology. The n and m parameters can take different values according to the crystallization process; $n_o = m + 1$ if the nucleation takes place during thermal analysis, $n_o = m$ if the nucleation rate is zero during the analysis and $n_o = m = 1$ if surface

crystallization is the predominant mechanism [17–19]. As an example plot of ln[–ln (1–X)] versus 1000/T for $Ge_{10}Se_{70}Sn_{20}$ glassy sample at different heating rates is shown in Figure 4. It is observed from Figure 4 that, the plots are linear over a wide temperature range. At higher temperatures a break is seen in the linearity for all heating rates. This break may be considered due to the saturation of the nucleation sites at the final stage of crystallization. The activation energy of crystallization has been calculated from the slope of plots of ln[–ln (1–X)] versus 1000/T and listed in Table 1.

Table 2: *Values of Avrami Exponent (n_o) and Dimensionality of Growth (m) for $Ge_{30-x}Se_{70}Sn_x$ (8≤x≤20) Glassy Samples using the Matusita Model; Value of Frequency Factor $K_o(sec^{-1})$ for these Glassy Samples using Augis – Bennett.*

Sn (at%)	Matusita model		Anguis- Bennett model
	n_o	m	$K_o(sec^{-1})$
8	2.97	2	8.21×10^{11}
11	2.98	2	1.74×10^{12}
14	3.08	2	2.56×10^{12}
17	2.90	2	2.96×10^{12}
20	3.09	2	8.1×10^{12}

Figure 5 shows linear plots of ln [–ln (1–X)] versus lnβ at three fixed temperatures for $Ge_{10}Se_{70}Sn_{20}$ glass sample. The value of n_o has been calculated from the slopes of the straight lines of Figure 5 and average value of n_o has been listed in Table 2. A noninteger value of n_o indicates that two crystallization mechanisms were working during the amorphous-crystalline transformation. It is observed that $n_o \neq m$, therefore $m = n_o - 1$. Accordingly, all the glassy materials predominantly crystallize in two dimensions suggesting surface and bulk nucleation.

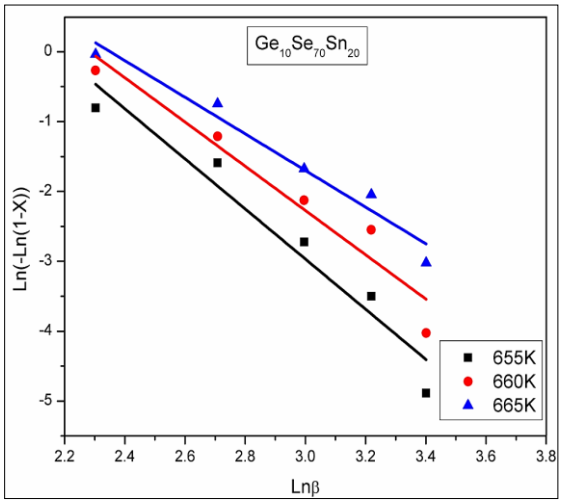

Fig. 5: *Plots of Ln [–ln (1–X)] vs. ln β $Ge_{10}Se_{70}Sn_{20}$ Glass.*

The activation energy of crystallization of glassy alloys has also been evaluated through the technique derived by **Gao-Wang** based on the Johnson–Mehl–Avrami equation and the Henderson equation. In this model, it is assumed that the nucleation is randomly distributed and the growth rate of the new phase depends on the temperature.

The theory of Gao and Wang is given by the following relationship [20,21]:

$$Ln\left(\frac{dX}{dt}\right)_p = constant - \frac{E_c}{RT_p} \qquad (3)$$

where, $\left(\frac{dX}{dt}\right)_p$ is the rate of volume fraction crystallized at the peak of crystallization temperature T_p, which is proportional to exothermic peak height. Plot of $Ln\left(\frac{dX}{dt}\right)_p$ versus $1000/T_p$ for Ge_{30-x} $Se_{70}Sn_x$ (8≤x≤20) is shown in Figure 6.

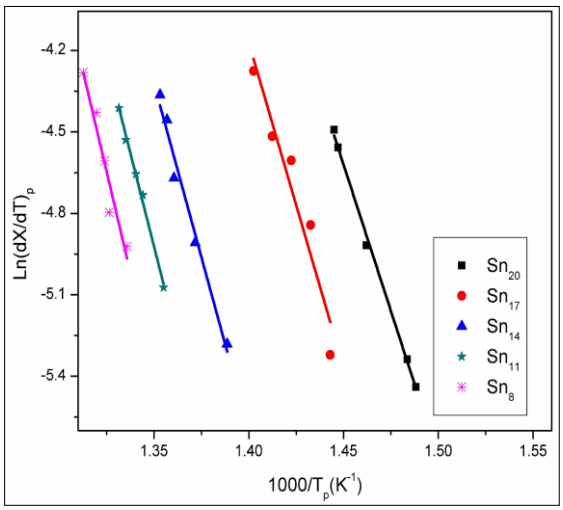

Fig. 6: *Plots of Ln $(dX/dt)_p$ vs. $1000/T_p$.*

The slope of curves (straight lines) gives the activation energy of crystallization (E_c). It is clear from Figure 7 that the peak height increases and shifts towards higher temperature values with the increase in heating rate. This is due to the fact that the heating rate increases from 10 to 30 $Kmin^{-1}$, more volume fraction of glass is crystallized in a smaller time as compared to the low heating rate.

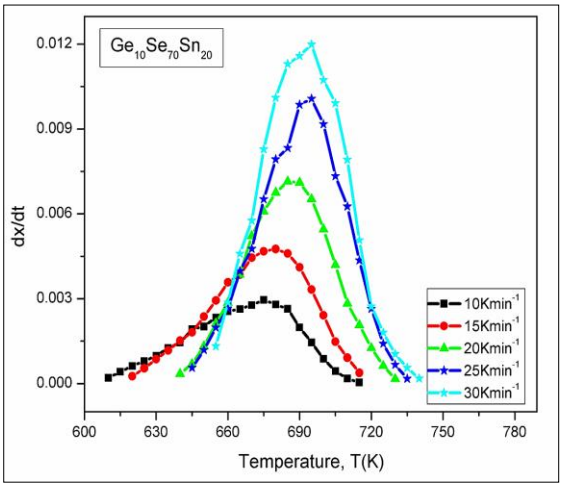

Fig. 7: *Plots of dX/dt vs. Temperature for $Ge_{10}Se_{70}Sn_{20}$ Glass.*

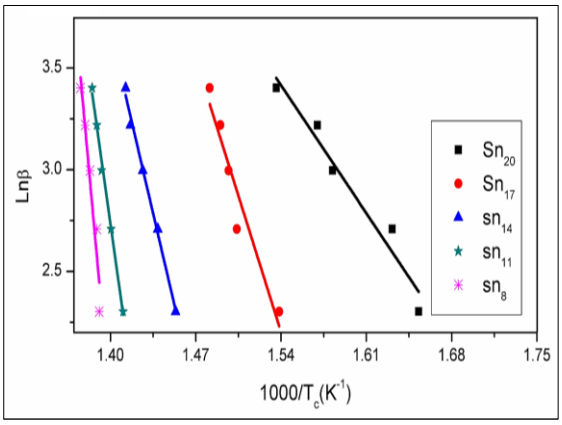

Fig. 8: *Plots of Ln β against 1000/T_c.*

The activation energy of crystallization E_c has been calculated from the variation of the onset crystallization temperature T_c with the heating rate using **Ozawa's** formulation [22]:

$$Ln\,\beta = Constant - \frac{E_c}{RT_c} \qquad (4)$$

Plot of ln β against 1000/T_c for Ge_{30-x} $Se_{70}Sn_x$ ($8 \le x \le 20$) glassy alloys is shown in Figure 8. The curves are found to be linear for different Sn contents. The activation energy of crystallization E_c is obtained from the slope of these plots and listed in Table 1. The activation energy for crystallization E_c, frequency factor (K_o) has been evaluated through the model suggested by Augis and Bennett [23]:

$$Ln\left(\frac{\beta}{T_c}\right) = LnK_o - \frac{E_c}{RT_c} \qquad (5)$$

where, T_c is onset crystallization temperature and K_o is the frequency factor (1/sec).

This equation shows that there exists a linear relation between ln (β/T_c) and 1000/T_c. The slopes of the resulting straight lines give the values of E_c, as shown in Figure 9 for Ge_{30-x} $Se_{70}Sn_x$ ($8 \le x \le 20$) glasses, while the intercepts with the vertical axis give the values of K_o. The value of K_o provides information for the calculation of number of nucleation site, present in the material for crystal growth. The values of K_o for different compositions are given in Table 2. The minimum value of K_o confirms the fact that glass is most stable, as the number of attempts made by nuclei's to cross the barrier are lowest for a glass. Number of attempts made by nuclei's reduces with decreasing percentage of Sn, suggesting increase in the stability of glasses. Also the result of frequency factor indicates that the glass forming ability increases with the decrease of Sn contents in the alloy which is again a signature of the increase of the stability of glass.

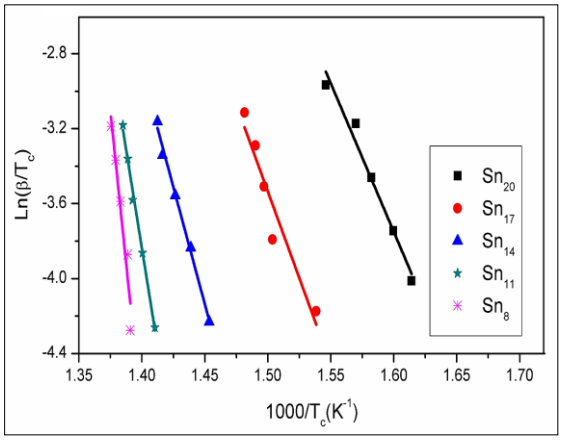

Fig. 9: *Plots of Ln (β/T_c) vs. 1000/T_c.*

A study of the results for the crystallization parameters supplied by the different isokinetic methods used shows considerable difference. This may be due to different approximations that have been adopted while arriving at the final equation of the various formalisms. It has

been observed from Table 1 that the values of activation energy are different for different models for each glassy system. It is clear that activation energy of crystallization decreases with the increase of the percentage of Sn. This suggests that crystallization rate decreases with increasing percentage of Sn. Therefore one can conclude that stability of sample decreases with increasing concentration of Sn.

Analysis of Variation of Volume of Fraction Crystallized (X) with Time of Crystallization

The experimental T-axis can be converted into t-axis using following equation [24]:

$$t = \frac{T - T_c}{\beta} \qquad (6)$$

where, T_c, onset crystallization temperature. X-T plot of $Ge_{10}Se_{70}Sn_{20}$ has been shown in Figure 10 and Figure 11 shows the converted crystallization kinetics curves of X-T curves to X-t curves for $Ge_{10}Se_{70}Sn_{20}$ at different heating rates. All observed X-t curves are shifted towards the lower crystallization times, with increasing heating rates, indicating the increased rate of nucleation.

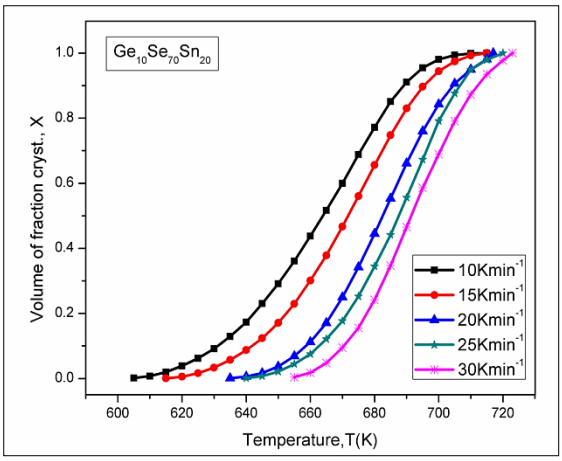

Fig. 10: *Plots of Volume of Fraction Crystallized (X) vs. Temperature for $Ge_{10}Se_{70}Sn_{20}$ Glass.*

The half-time of crystallization $t_{1/2}$, is defined as the elapsed time from the onset of crystallization until the crystallization reaches half of the whole crystallization contribution. It can be obtained directly from X-t curves as shown in Figure 11 for $Ge_{10}Se_{70}Sn_{20}$ glassy alloy. Generally, the rate of crystallization can be described as the reciprocal of $t_{1/2}$ [25]. The value of $t_{1/2}$ and reciprocal of $t_{1/2}$ have been listed in Table 3.

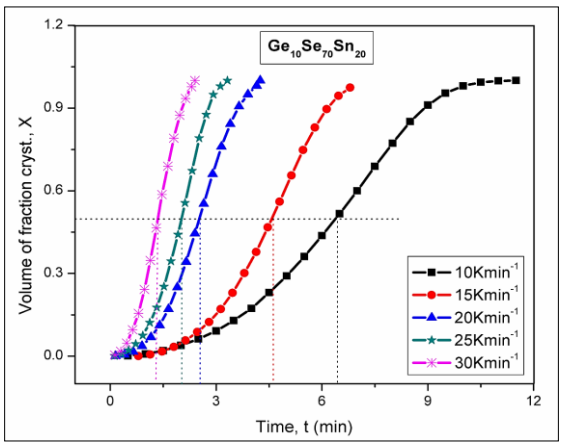

Fig. 11: *Plots of Volume of Fraction Crystallized (X) vs. Time for $Ge_{10}Se_{70}Sn_{20}$ Glass.*

It has been seen from Table 3 that the larger half-time of crystallization indicates a slower crystallization rate. It has also been observed that $t_{1/2}$ decreases with increasing heating rate as well as decreasing Sn content. The variation of $t_{1/2}$ with concentration of Sn content has been shown in Figure 12.

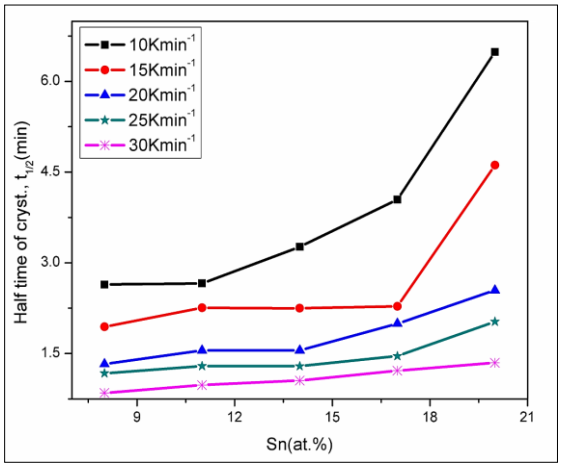

Fig. 12: *Plots of Volume of Fraction Crystallized (X) vs. Sn at %.*

Generally, the Avrami model is used to illustrate the isothermal crystallization kinetics. It has also been employed to explain the non-isothermal crystallization of semi-crystalline materials. The mathematical formulation of Avrami model can be expressed as follows [26]:

$$X = 1 - \exp(-Kt^{n_a}) \qquad (7)$$

This equation can be rearranged in the form of double logarithmic:

$$Ln\left[-Ln\left(1 - X(t)\right)\right] = LnK + n_a Lnt \qquad (8)$$

where, n_a is the Avarmi exponent depending on the nucleation and growth process, K is the crystallization rate constant. The kinetic parameter n and K have been obtained from the slope and intercept of the line, respectively, from the plot of Ln[-Ln(1-X)] versus Lnt, as shown in Figure 13. Jeziorny [27] pointed out that the value of the rate constant K should be corrected for the rate of crystallization depends on the heating rate employed. Considering the influence of various heating rates on the non-isothermal crystallization condition, Jeziorny gave the final form of the parameter characterizing the kinetics of non-isothermal crystallization as:

$$LnK_c = \frac{LnK}{\beta} \quad (9)$$

where K_c, is the modified crystallization rate factor. The values of n_a, K and K_c have been listed in Table 4.

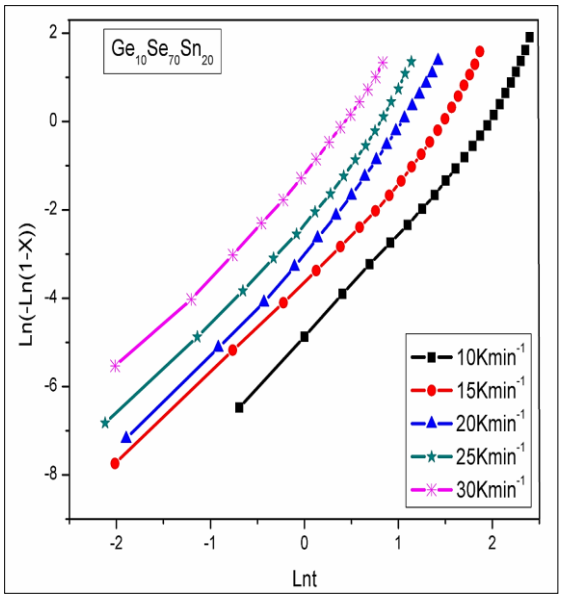

Fig. 13: *Plots of Ln [–ln (1–X)] vs. Lnt for $Ge_{10}Se_{70}Sn_{20}$ Glass.*

Table 3: *Values of Half-time of Crystallization, $t_{1/2}$(min) and Reciprocal of Half-time of Crystallization, $1/t_{1/2}$(min^{-1}) for $Ge_{30-x}Se_{70}Sn_x$ ($8 \le x \le 20$) Glassy Alloys using X-t Curves.*

Heating rate (βKmin^{-1})	Sn_8		Sn_{11}		Sn_{14}		Sn_{17}		Sn_{20}	
	$t_{1/2}$	$1/t_{1/2}$	$t_{1/2}$	$1/t_{1/2}$	$t_{1/2}$	$1/t_{1/2}$	$t_{1/2}$	$1/t_{1/2}$	$t_{1/2}$	$1/t_{1/2}$
10	2.641	0.379	2.66	0.376	3.264	0.306	4.046	0.247	6.488	0.154
15	1.942	0.515	2.256	0.443	2.249	0.445	2.281	0.438	4.616	0.217
20	1.325	0.754	1.553	0.644	1.551	0.645	1.699	0.501	2.545	0.393
25	1.723	0.853	1.293	0.773	1.291	0.775	1.451	0.686	2.026	0.494
30	0.847	1.180	0.979	1.022	1.053	0.949	1.216	0.823	1.348	0.742

It has been seen that the difference arises between the values of avrami exponent n_o and n_a, calculated from Matusita model and Avrami model, respectively. This difference arises due to the different type of mathematical formulation of models. It has also been observed that the value of K_c increase with increasing heating rate, suggesting that the glassy sample crystallized faster when heating rate increases. In addition the K_c values increases with decreasing Sn concentration. These results are consistent with the observation based on the half-time of crystallization.

Mo et al. [25, 28,29] proposed a different kinetic equation by combining the Avrami and Ozawa equations for characterization of non-isothermal crystallization assuming that the non-isothermal crystallization procedure comprises of infinitesimally small isothermal crystallization steps or pseudo-isothermal processes i.e., the volume of fraction crystallized is correlated to the heating rate and crystallization time.

The Ozawa equation [30] is a modification of the Avarmi equation which considers the effect of heating rate on crystallization from the melt and replaces the crystallization time under isothermal conditions with heating rate as follows:

$$X = 1 - \exp\left(-\frac{K(T)}{\beta^{m'}}\right) \quad (10)$$

This equation can be rearranged in the form of double logarithmic form:

$$Ln\left[-Ln\left(1 - X(t)\right)\right] = LnK(T) - m' Ln\beta \quad (11)$$

By rearrangement of Eqs. (8) and (11) at a given volume of fraction crystallized, the combination of these two models derives a new kinetics equation for the non- isothermal crystallization:

$$Ln\beta = LnF(T) - \alpha Lnt \quad (12)$$

where, parameter $F(T) = [K(T)/K]^{1/m'}$ refers to the value of the heating rate when the system reaches a certain degree of crystallinity in the unit time. LnF(T) has a definite physical implication, that is, the higher the value of LnF(T), the slower the crystallization rates [30]. α is the ratio of the Avrami exponent n_a to the Ozawa exponent m'.

Table 4: *Values of Avrami Exponent (n_a), Avrami Crystallization Rate Constant, K(min^{-1}) and Modified Crystallization Rate Factor, $K_c(K^{-1})$ for $Ge_{30-x}Se_{70}Sn_x$ ($8 \leq x \leq 20$) Glassy Samples using Avrami Model.*

Sn (at%)	Heating rate βKmin^{-1}	Avrami model		
		n_a	K(min^{-1})	$K_c(k^{-1})$
Sn_8	10	2.52	0.1435	0.8236
	15	1.58	0.1641	0.8865
	20	1.82	0.4539	0.9613
	25	2.61	0.5099	0.9734
	30	1.92	1.0097	1.0003
Average		**2.09**	**0.4562**	**0.9290**
Sn_{11}	10	2.08	0.1009	0.7950
	15	2.27	0.1066	0.8613
	20	2.09	0.3016	0.9418
	25	2.86	0.3755	0.9616
	30	2.17	0.8206	0.9934
Average		**2.29**	**0.3410**	**0.9106**
Sn_{14}	10	2.43	0.03821	0.7214
	15	2.54	0.0929	0.8535
	20	2.17	0.2589	0.9347
	25	2.38	0.3742	0.9614
	30	2.1	0.5979	0.9830
Average		**2.32**	**0.2724**	**0.8908**
Sn_{17}	10	2.65	0.01871	0.6717
	15	2.33	0.1141	0.8653
	20	2.31	0.2124	0.9255
	25	2.42	0.3080	0.9539
	30	2.36	0.4667	0.9749
Average		**2.41**	**0.2239**	**0.8783**
Sn_{20}	10	2.65	0.0063	0.6028
	15	2.38	0.0304	0.7924
	20	2.62	0.0643	0.8718
	25	2.52	0.1308	0.9219
	30	2.43	0.3600	0.9665
Average		**2.52**	**0.1184**	**0.8311**

Table 5: *Values of LnF(T) and α at Different Volume of Fraction Crystallized (X) for $Ge_{30-x}Se_{70}Sn_x$ ($8 \leq x \leq 20$) Glassy Samples using Mo′s Approach.*

.

volume fraction of cryst., X	Sn_8		Sn_{11}		Sn_{14}		Sn_{17}		Sn_{20}	
	LnF (T)	A	LnF (T)	α	LnF (T)	α	LnF (T)	α	LnF (T)	α
0.2	2.835	0.97	2.976	1.05	3.02	0.86	3.13	0.92	3.35	0.69
0.4	3.188	0.97	3.294	0.94	3.26	0.92	3.42	0.91	3.58	0.71
0.6	3.386	0.95	3.533	1.03	3.58	1.02	3.68	0.99	3.75	0.73
0.8	3.561	0.93	3.687	0.98	3.77	1.00	3.79	0.91	3.87	0.74

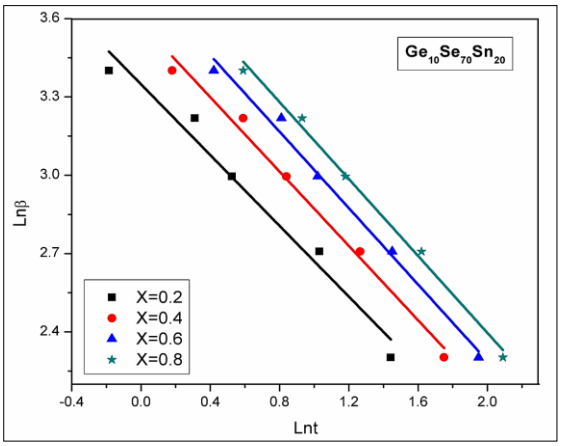

Fig. 14: *Plots of Ln β vs. Lnt for $Ge_{10}Se_{70}Sn_{20}$ Glass.*

The importance of this method is that it correlates the heating rate to temperature and time of crystallization. According to Eq. (12), at a given degree of crystallinity, the plots of lnβ versus lnt give a straight line with LnF (T) as the intercept and α as the slope, as shown in Figure 14. The obtained LnF(T) and α values listed in Table 5. It has been observed the LnF(T) values gradually increases with the increase of volume of fraction crystallized (X) and decrease with decreasing the concentration of Sn. The value of LnF(T) is found to be minimum for the glassy alloy $Ge_{22}Se_{70}Sn_8$.

CONCLUSION

The study of kinetics of crystallization for Ge-Se-Sn ternary chalcogenide glassy system with variation of Sn concentration has been carried out. Our investigations show the following notable features:

1. The activation energy of crystallization decreases with the increase of the percentage of Sn. This suggests that crystallization rate decreases with increasing percentage of Sn. Therefore, one can conclude that stability of sample decreases with increasing concentration of Sn.
2. There is a decrease in Frequency Factor as the Sn concentration decreases. These results indicate that the glass forming ability increases with decreasing Sn content.
3. The half –time of crystallization decreases with increasing heating rate and the crystallization rate constant increases with increasing heating rate i.e., glassy materials crystallized faster when the heating rate increased.
4. It has been found that Ln F(T) increases with increasing volume of fraction crystallized (X) and decreases with decrease of Sn concentration in the series of Ge-Se-Sn system which again confirm above stated results.

ACKNOWLEDGEMENTS

The authors (Anusaiya Kaswan and Vandana Kaumari) are thankful to UGC, India for providing financial support in the form of UGC-BSR fellowship during this work.

REFERENCES

1. Bletskan D I, Glass Formation in Binary and Ternary Chalcogenide System, *Chalogenide lett.* 2006; 3: 81–119p.
2. Wuttig M, Yamada N, Phase-change Materials for Rewriteable Data Storage, *Nature Mater*. 2007; 6: 824–32p.
3. Pirovano A, Lacaita A, Electronic Switching in Phase-change Memories, *IEEE T Electr Devices*, 2004; 51: 452–59p.
4. Sousa V. Chalcogenide Materials and their Application to Non-Volatile Memories, *Microelectronic Eng*. 2011; 88: 807–13p.
5. Ohta T, Phase-change Optical Memory Promotes the DVD Optical Disk, *J Optoelectron. Adv Mater*. 2001; 3: 609–26p.
6. Khan S A, Zulfequar M, Husain M, Crystallization Kinetics of a-Ga_5Se_{95-x} Sb_x, *J Phys Chem Solids* 2002; 63:1787–96p.
7. Popescu M, Disordered Chalcogenide Optoelectronic Materials Phenomena and Applications, *J Optoelectron Adv Mater* 2005; 7: 2189–210p.
8. Mehta N, Applications of Chalcogenide Glasses in Electronics and Optoelectronics: A Review, *J Sci Ind Res*. 2006; 65: 777–86p.
9. Lafi OA, Imran MMA, Abudullah MK, *et al*. Thermal Characterization of Se_{100-x} Sn_x (x=4, 6 & 8) Chalcogenide Glasses using Differential Caloremetr, *Thermochemica Acta*, 2013; 560: 71–5p.
10. Kassem M, Coq DL, Boidin R, *et al*. New Chalcogenide Glasses in the CdTe-AgI-As_2Te_3 system, *Mater Res Bull*. 2012; 47: 193–8p.

11. Singh A K, A Short Over View on Advantage of Chalcogenide Glassy Alloys, *J Non-Oxide Glasses*, 2012; 3(1):1–4p.
12. Wang HR, Gao YL, Ye YF, *et al.* Crystallization Kinetics of an Amorphous Zr-Cu-Ni alloy: Calculation of the Activation Energy, *J Alloys Comp.* 2003; 353: 200–6p.
13. Kaswan A, Kumari V, Patidar D, *et al.* Kinetics of Crystallization of Ge_{30-x} $Se_{70}Sb_x$ (x=15, 20, 25) Chalcogenide Glasses, *Process Appl Ceramics*. 2013; 8(1): 25–30p.
14. Kissinger HE, Variation of Peak Temperature with Heating Rate in Differential Thermal Analysis, *J Res Nat Bur Stand.* 1956; 57 (4): 217–21p.
15. Kissinger HE, Reaction Kinetics in Differential Thermal Analysis, *J Res Nat Bur Stand.* 1957; 29 (11): 1702–6p.
16. Matusita K, Konatsu T, Yokota R, Kinetics of Non-isothermal Crystallization and Activation Energy for Crystal Growth in Amorphous Materials, *J Mater Sci.* 1984; 19: 291–96p.
17. Çelikbilek M, Ersundu AE, Solak N, *et al.* Crystallization Kinetics of the Tungsten-tellurite Glasses, *J Non-Cryst. Solids*. 2011; 357: 88–95p.
18. Çelikbilek M, Ersundu AE, Aydın S, in: Y. Mastai (Ed.), *Advances in Crystallization Processes*, In tech, 2012; 127–62p.
19. Yardımcı D, Çelikbilek M, Ersundu AE, *et al.* Thermal and Micro-structural Characterization and Crystallization Kinetic Studies in the TeO_2-B_2O_3 System, *Mater Chem Phys.* 2013; 137: 999–1006p.
20. Gao YQ, Wang W, On the Activation Energy of Crystallization in Metallic Glasses, *J Non-Cryst. Solids*, 1986; 81: 129–34p.
21. Henderson DW, Thermal Analysis of Non-isothermal Crystallization Kinetics in Glass Forming Liquid, *J Non-Cryst. Solids*, 1979; 30: 301–15p.
22. Saxena NS, Phase Transformation Kinetics and Related Thermodynamic and Optical Properties in Chalcogenide Glasses, *J Non-Cryst Solids*. 2004; 345: 161–68p.
23. Augis JA, Bennett JE, Calculation of Avrami Parameters for Heterogenous Solid State Reaction using a Modification of the Kissinger Method, *J Therm Anal Calor*. 1978; 13: 283–92p.
24. Pablick C, Ahrens B, Henke B, *et al.* Differential Scanning Calorimeter Investigations on Eu-doped Fluorozirconate-based Glass Ceramics, *J Non-Cryst Solids*. 2010; 356: 3085–89p.
25. Marinovic M, Jankovic B, Milicevic B, *et al.* The Comparative Kinetic Analysis of the Non-isothermal Crystallization Process of Eu^{3+} doped $Zn_2S_iO_4$ Powders Prepared via Polymer Induced Sol-gel Method, *Powder Tech.* 2013; 249: 497–512p.
26. Avrami M, Kinetics of Phase Change II Transformation-time Relations for Random Distribution of Nuclei, *J Chem Phys*. 1940; 8: 212p.
27. Jeziorny A, Parameters Characterizing the Kinetics of the Non-isothermal Crystallization of Poly(ethylene terephthalate) determined by DSC, *Polymer*, 1978; 19: 1142p.
28. Lio M, Zhao Q, Wang Y, *et al.* Melting Behaviors Isothermal and Non-isothermal Crystallization Kinetics of Nylon1212, *Polymer*, 2003; 44: 2537–45p.
29. Jiang C, Wang D, Zhang M, *et al.* Effect of Highly Filled Ferrites on Non-isothermal Crystallization Behavior of Polyamide 6 Bonded Ferrites, *Eur. Polym J.* 2010; 46: 2206–15p.
30. Ozawa T. Kinetics of Non-isothermal Crystallization, *Polymer*, 1971; 12: 150–8p.

Cite this Article

Anusaiya Kaswan, Vandana Kumari, Patidar D et al. Kinetics of non-isothermal crystallization of Ge-Se-Sn Chalcogenide Glasses, *Research & Reviews: Journal of Physics (RRJoPHY)* 2015; 4(2): 25–34p.